

Coexistence of Real-Time Source Reconstruction and Broadband Services Over Wireless Networks

Anup Mishra*, Nikolaos Pappas†, Čedomir Stefanović*, Onur Ayan‡, Xueli An‡,
Yiqun Wu‡, Petar Popovski*, and Israel Leyva-Mayorga*

*Department of Electronic systems, Aalborg University, Denmark ({anmi, cs, petarp, ilm}@es.aau.dk)

†Linköping University, Linköping, Sweden (nikolaos.pappas@liu.se)

‡Huawei Technologies, Munich, Germany ({onur.ayan, xueli.an, wuyiqun}@huawei.com)

Abstract—Achieving a flexible and efficient sharing of wireless resources among a wide range of novel applications and services is one of the major goals of the sixth-generation of mobile systems (6G). Accordingly, this work investigates the performance of a real-time system that coexists with a broadband service in a frame-based wireless channel. Specifically, we consider real-time remote tracking of an information source, where a device monitors its evolution and sends updates to a base station (BS), which is responsible for real-time source reconstruction and, potentially, remote actuation. To achieve this, the BS employs a grant-free access mechanism to serve the monitoring device together with a broadband user, which share the available wireless resources through orthogonal or non-orthogonal multiple access schemes. We analyse the performance of the system with time-averaged reconstruction error, time-averaged cost of actuation error, and update-delivery cost as performance metrics. Furthermore, we analyse the performance of the broadband user in terms of throughput and energy efficiency. Our results show that an orthogonal resource sharing between the users is beneficial in most cases where the broadband user requires maximum throughput. However, sharing the resources in a non-orthogonal manner leads to a far greater energy efficiency.

I. INTRODUCTION

Real-time autonomous and cyber-physical systems have attracted significant attention over the past decade due to their broad range of time-critical applications such as autonomous transportation and industrial automation [1], [2]. These systems have devices, often geographically distributed, monitoring an information source or a process and sending updates to a remote monitor and/or digital twin. The objective of such systems is real-time tracking and reconstruction of the source process at the monitor receiving the updates, which enables decision-making and actuation [1]. Several metrics, such as mean square estimation error, age-of-information (AoI) and its variants, etc., have been studied as performance measures for remote tracking [2], [3]. These metrics, however, are oblivious to the semantics of information (i.e., significance, goal-oriented usefulness, and contextual value) and its impact on the overall cyber-physical system [1], [4], [5]. To address this problem, recent works introduced metrics such as real-time reconstruction error and cost of actuation error, which account for the semantics of information transmitted and capture different aspects of the system performance [1], [6].

This work is a joint contribution by members of Working Item 205 on “6G Radio Access” of the one6G association.

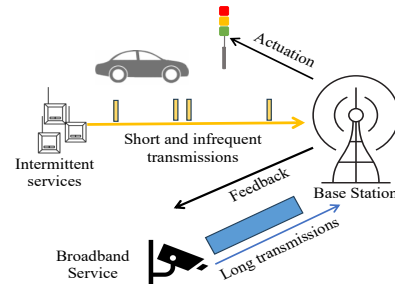


Fig. 1. A representative uplink scenario with a BS serving an intermittent user and a broadband user.

Studies on real-time remote tracking typically consider that updates from a device are followed by feedback from the monitor, in the form of an acknowledgement (ACK) or negative ACK (NACK). Moreover, these often rely on the ‘idealistic’ assumptions of always having wireless resources available for transmitting updates and instantaneous feedback [1]. However, such assumptions are unrealistic, as these would require an exorbitant wastage of radio resources, particularly given the intermittent nature of device transmissions in real-time autonomous systems [7]. Specifically, major challenges in wireless communication systems include the long access delay and overhead in grant-based access mechanisms, the inefficient radio resource utilization in grant-free access mechanisms, and the delayed transmission of the update or feedback in frame-based transmissions [7], [8]. The massive number of heterogeneous devices in future wireless networks, such as the sixth-generation of mobile systems (6G), is going to exacerbate these challenges further. Consequently, the performance of real-time remote reconstruction must be investigated in resource sharing communication scenarios that do not rely on idealistic assumptions. Moreover, the analysis must account for relevant performance metrics, the user distribution across service types, and the multiple access mechanisms that allocate resources to each service [6], [8], [9].

Motivated by the above discussion, in this work we consider an uplink scenario where a device is monitoring an information source and sending updates to a base station (BS), which tracks and reconstructs the source process in real-time. Fig. 1 illustrates such a scenario, where devices can be utilized for near real-time traffic monitoring via a digital twin, and real-time actuation of traffic signals. Due to its intermittent behaviour, we consider that the monitoring device transmits

its updates to the cellular network through a grant-free access mechanism. For ease of exposition, we will henceforth refer to this device as the *intermittent user*. The BS allocates available wireless resources among the intermittent user and a broadband user that generates data continuously [7], [8]. Moreover, a frame-based communication model is considered, where uplink and downlink transmissions are multiplexed in time. For the considered model, we analyse the performance metrics of the intermittent user and compare them with those obtained from the model employed in conventional studies on real-time remote tracking. To this end, we consider time-averaged reconstruction error (TRE), time-averaged cost of actuation error (TCAE) and update-delivery cost (UC) as performance metrics for the intermittent user. Here, we define UC as the average number of re-transmissions needed to successfully deliver an update. We show that the desirably low TRE and TCAE performance of the communication model in conventional studies is achieved at the expense of a disproportionately high UC. We then study performance trade-offs between the intermittent user and the broadband user, whose metrics are throughput and energy efficiency, by sharing the available wireless resources using frequency division multiple access (FDMA) and non-orthogonal multiple access (NOMA) schemes. We show that NOMA achieves a better performance trade-off between the two users, particularly when energy efficiency is the performance measure for the broadband user.

II. SYSTEM MODEL

We consider an uplink scenario wherein a broadband user and an intermittent user are allocated wireless resources to communicate with the BS. The users and the BS are equipped with a single antenna. The users are indexed by $m \in \{1, 2\}$, with the broadband user indexed as $m = 1$ and the intermittent user as $m = 2$. The available wireless resources are within a frequency band of bandwidth B Hz [7]. This bandwidth B is divided into three sub-bands: 1) B_1 reserved for the broadband user, 2) B_2 reserved for the intermittent user, and 3) B_3 to be shared by both users, such that $B_1 + B_2 + B_3 = B$. Let $\alpha_{m,i} \in \{0, 1\}$ indicate the allocation of user m to sub-band $i \in \{1, 2, 3\}$, such that $\alpha_{m,i} = 1$ if user m is assigned to sub-band i , and $\alpha_{m,i} = 0$ otherwise. We consider a time-slotted communication system with T_s as the duration of each slot. The communication is segmented into frames, with each frame consisting of T_F consecutive time slots. Subsequently, we detail the multiple access schemes as follows.¹

- 1) *FDMA*: Users are allocated non-overlapping frequency sub-bands, with B_1 containing slots reserved for the broadband user and B_2 for the intermittent user. Hence, signal overlap between the users is avoided by setting $\alpha_{1,1} = \alpha_{2,2} = 1$, $B = B_1 + B_2$, and $B_3 = 0$ [7].
- 2) *NOMA*: Both users are allocated the entire bandwidth by setting $\alpha_{1,3} = \alpha_{2,3} = 1$, $B_1 + B_2 = 0$ and $B_3 = B$.

¹We exclude time division multiple access (TDMA) because it either restricts the choice of the sampling policy or renders the analysis intractable, requiring joint design of both the sampling policy and resource allocation.

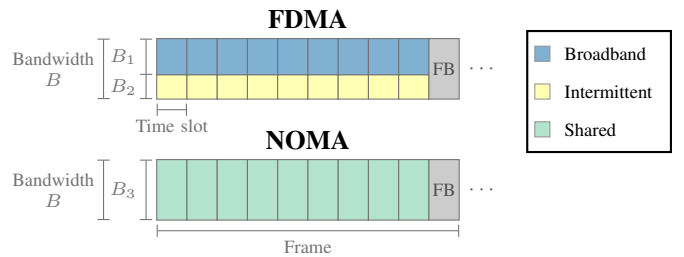


Fig. 2. Considered frame structure with FDMA and NOMA.

This leads to a complete signal overlap between the users when both transmit in the same time slot [7].

A. Transmission Model

The first $T_F - 1$ slots are reserved for uplink transmission, while the last slot is reserved for downlink transmission to provide feedback, ACK or NACK, to the users from the BS. Here, the time slots and frames are indexed by $t \in \{0, 1, \dots\}$ and $f \in \{0, 1, \dots\}$, respectively. Fig. 2 illustrates the frame structure with FDMA and NOMA schemes [7]. Next, we outline the transmission policy of the broadband user and the intermittent user, respectively.

1) *Broadband user*: The user segments its transmit data into packets and employs a forward error correction (FEC) mechanism using an ideal rate-less packet-level coding, wherein blocks of K source packets are encoded into blocks of linearly independent packets. An encoded block can span over multiple frames. Subsequently, the BS is able to decode a block of source packets once it has successfully received K encoded packets representing the source block. Successful/failed decoding of a source block is informed to the user by the BS using feedback at the end of a frame. If the user receives an ACK through feedback, then the user proceeds to transmit encoded packets of the next source block, otherwise, the user keeps transmitting the encoded packets of the current source block. Such transmission strategy ensures that the broadband user is guaranteed to achieve reliability 1.

2) *Intermittent user*: We model the information source at the user by an ergodic two-state discrete-time Markov chain (DTMC) $\{X_t, t \in \mathbb{Z}_0^+\}$, where the state X_t of the source at time slot t can be 0 or 1 [1]. In this model, the states represent distinct sets of values collected from one or multiple sensors, aggregated at a single communication device which, for ease of exposition, are simply denoted as 0 or 1 in the two-state DTMC [1]. The self-transition probabilities for states 0 and 1 are denoted as $1 - p_s$ and $1 - q_s$, respectively. As a result, $\mathbb{P}(X_{t+1} = X_t) = \mathbb{1}(X_t = 0)(1 - p_s) + \mathbb{1}(X_t = 1)(1 - q_s)$, with $\mathbb{1}(\cdot)$ denoting the indicator function. The user observes the process X_t and informs the BS about its state by sending updates over a wireless channel. To that end, the user will generate an update X_t through sampling, and transmit the update to the BS in a data packet of length L . Note that the structure of the frame, illustrated in Fig. 2, allows for the instantaneous transmission of an update only in the first $T_F - 1$ slots of the frame. Moreover, we assume that the intermittent user has a transmission queue of length 1, so

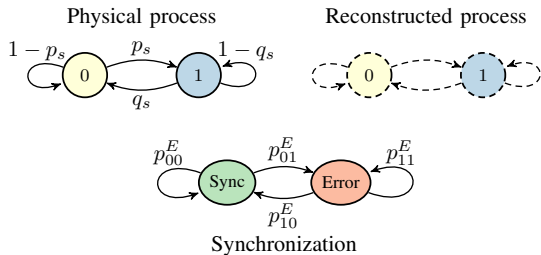


Fig. 3. Two-state DTMC of the physical process being monitored, its reconstruction at the BS, and the state of the system vis-à-vis synchronization.

any new update replaces the previous packet in the queue. The actions of sampling and transmission at time slot t are denoted by $\alpha_t^s \in \{0, 1\}$ and $\alpha_t^{\text{tx}} \in \{0, 1\}$, respectively, where $\alpha_t^a = 1$, $a \in \{s, \text{tx}\}$, indicates that the action is taken at time slot t , and $\alpha_t^a = 0$ otherwise. Next, if the BS successfully receives the packet, it updates the state of the reconstructed source instantaneously. The feedback from the BS to the intermittent user, and subsequently the re-transmission of the failed update, depends on the sampling policy employed for process monitoring (see Section IV). Notwithstanding, if the sampling policy requires feedback and multiple updates are sent within a frame, feedback will be provided only for the latest update. Fig. 3 illustrates the process monitoring of the considered source process. As highlighted in Section I, the reconstructed process at the BS can be utilized to construct a digital twin or effectuate real-time actuation.

B. Physical Layer Model

We denote the channel coefficient between the BS and user m at time slot t as $h_{m,t} \in \mathbb{C}$. The channel coefficient is modeled as a random variable that accounts for large-scale and small-scale fading losses. The small-scale fading loss is modeled as a circularly symmetric complex Gaussian (CSCG) random variable with zero mean and unit variance. On the other hand, the large-scale fading loss is a function of the speed of light c , the carrier frequency f_c , the distance between the BS and user m , d_m , the path loss exponent η , and the antenna gains at the BS and the user, G_b and G_m , respectively. Thus, the large-scale fading loss, β_m , can be computed as

$$\beta_m = \mathbb{E}\{|h_{m,t}|^2\} = \frac{G_m G_b c^2}{(4\pi f_c)^2 d_m^\eta}, \quad m \in \{1, 2\}. \quad (1)$$

By $x_{m,t} \in \mathbb{C}$ we denote as the transmit signal between user m and the BS at time slot t , and by $P_{m,t} \in [0, P_{\max}]$ as the transmission power of user m . Subsequently, the received signal at the BS during uplink transmission in the i -th sub-band and t -th time slot can be written as

$$y_{i,t} = h_{1,t} x_{1,t} \alpha_{1,i} + h_{2,t} x_{2,t} \alpha_{2,i} + w_{i,t}, \quad \forall i \in \{1, 2, 3\}, \quad (2)$$

where $w_{i,t}$ is the CSCG distributed additive noise with zero mean and variance $\sigma_i^2 = B_i \kappa T_w 10^{N_f/10}$. Here, κ is the Boltzmann constant, T_w is the system noise temperature, and N_f is the noise figure in dB. Hence, the signal-to-interference

plus noise ratio (SINR) for the signal of user m in the i -th sub-band and t -th time slot can be computed as

$$\gamma_{m,i,t} = \frac{|h_{m,t}|^2 P_{m,t} \alpha_{m,i}}{|h_{n,t}|^2 P_{n,t} \alpha_{n,i} + \sigma_i^2}, \quad m, n \in \{1, 2\} \wedge m \neq n. \quad (3)$$

Assuming the interference can be treated as Gaussian noise, we define a threshold for decoding the signal of user m at time slot t in sub-band i as the function of the rate r_m , as

$$\gamma_{m,i}^{\min}(r_m) = 2^{r_m/B_i} - 1, \quad (4)$$

such that if $\gamma_{m,i,t} \geq \gamma_{m,i}^{\min}(r_m)$, then the packet of user m is successfully decoded at time slot t ; we denote the corresponding probability of successful decoding by

$$p_{m,i,t} = \mathbb{P}(\gamma_{m,i,t} \geq \gamma_{m,i}^{\min}(r_m)). \quad (5)$$

Further, we introduce the error probability for user m as $\epsilon_{m,i}$, defining it as the probability of a transmission error in the absence of interference from the other user $n \neq m$, given by

$$\epsilon_{m,i} = \mathbb{P}(\gamma_{m,i,t} \leq \gamma_{m,i}^{\min}(r_m) : \alpha_{m,i} = 1 \wedge P_{n,t} \alpha_{n,i} = 0). \quad (6)$$

The BS aims to decode the received signals instantaneously, i.e., in the same time slot it received the packet. While decoding the signal of user m in the FDMA regime is straightforward, we consider a successive interference cancellation (SIC) decoder in conjunction with the *capture effect* for NOMA [7], [8]. The success or failure of the decoding process is dictated by the SINR defined in (3). The BS attempts to decode the received signal and, if successful, applies SIC to decode the remaining signal (if any), ensuring both users can be decoded if the SINR and signal-to-noise ratio (SNR) thresholds are met.

III. PERFORMANCE METRICS

In this section, we derive the expression for metrics relevant to the performance of the broadband and intermittent user.

A. Broadband User

For the broadband user, we consider throughput and energy efficiency to be the performance metrics. To this end, the transmission rate r_1 is selected as the minimum of: 1) the maximum rate r_1^{\max} and 2) the maximum achievable data rate for the target error probability ϵ_1^* , expressed as

$$r_1 = \max\{r \in (0, r_1^{\max}) : \epsilon_{1,i}(r) = \epsilon_1^*, P_{1,t} \leq P_m^{\max}\}. \quad (7)$$

For the desired rate r_1 and the target error probability ϵ_1^* , $P_{1,t}$ can be calculated by assuming absence of interference in (3) and then utilizing equations (6) and (5), given by

$$P_{1,t} = \min\left(\frac{(2^{r_1/B_i} - 1) \sigma_i^2}{\mathbb{E}[|h_1|^2] \log(\epsilon_1^* - 1)}, P_{\max}\right), \quad (8)$$

where it is assumed that the broadband user has statistical knowledge of its channel, i.e., of $\mathbb{E}[|h_1|^2]$. Denoting the random variable of the number of frames needed to decode the block of K source packets transmitted by the user as $F(K)$, the throughput of the broadband user is calculated as

$$S_B = r_i K (T_F - 1) / (\mathbb{E}\{F(K)\} T_F), \quad (9)$$

and the energy efficiency is calculated as $S_B/P_{1,t}$.

B. Intermittent User

We consider context-dependent and cost-aware performance metrics for the intermittent user [1], [6]. These rely on the BS constructing an estimate of the original source state X_t at time slot t , denoted by \hat{X}_t . We consider that $\hat{X}_t = X_t$ whenever an update is received at time slot t and $\hat{X}_t = \hat{X}_{t-1}$ otherwise. These metrics are described in the following.

1) *TRE*: The real-time reconstruction error is calculated as $E_t = \mathbb{1}(X_t \neq \hat{X}_t) \in \{0, 1\}$ [1]. As shown in Fig. 3, E_t can be construed as an indicator for the state of the system, with $E_t = 1$ being the erroneous state and $E_t = 0$ being the synced state. Subsequently, for an observation interval of $[1, T_o]$, with T_o being a large number, the TRE is defined as

$$\bar{E} = \lim_{T_o \rightarrow \infty} \frac{1}{T_o} \sum_{t=1}^{T_o} E_t = \frac{1}{T_o} \sum_{t=1}^{T_o} \mathbb{1}(X_t \neq \hat{X}_t). \quad (10)$$

Interestingly, the evolution of E_t can be described by a Markov chain as well, as shown in Fig. 3; with transition probabilities defined as $p_{ji}^E = \mathbb{P}(E_{t+1} = j | E_t = i)$, $\forall i, j \in \{0, 1\}$. For ease of understanding, we derive the general expression of the transition probabilities p_{00}^E and p_{11}^E as follows.

$$p_{00}^E = \sum_{i=0}^1 \mathbb{P}(E_{t+1} = 0 | E_t = 0, X_t = i) \mathbb{P}(X_t = i), \quad (11)$$

with $\mathbb{P}(X_t = i) = \mathbb{1}(i = 0) \frac{q_s}{p_s + q_s} + \mathbb{1}(i = 1) \frac{p_s}{p_s + q_s}$, $\forall i \in \{0, 1\}$, calculated using stationary distribution of X_t . To compute (11), we first define an indicator event for successful decoding of a transmitted packet of the intermittent user as α^d such that $p_{2,i,t} = \mathbb{P}(\alpha_t^d = 1)$. Naturally, $\mathbb{P}(\alpha_t^d = 0) = 1 - p_{2,i,t}$. Next, with $j \in \{0, 1\}$, we denote probabilities of joint sampling, transmission, and decoding events at time $t + 1$ as $p_{\text{stx}}^j = \mathbb{P}(\alpha_{t+1}^s = 1, \alpha_{t+1}^{\text{tx}} = j)$, and $p_{\text{stx}}^{d_j} = \mathbb{P}(\alpha_{t+1}^s = 1, \alpha_{t+1}^{\text{tx}} = 1, \alpha_{t+1}^d = j)$; Section II-A2 delineates events α_t^s and α_t^{tx} in detail. Subsequently, we obtain

$$\mathbb{P}(E_{t+1} = 0 | E_t = 0, X_t = 0) = (1 - p_s) + p_s p_{\text{stx}}^{d_1}. \quad (12)$$

Similarly, $\mathbb{P}(E_{t+1} = 0 | E_t = 0, X_t = 1)$ can be calculated. In regard to p_{11}^E , we have

$$\mathbb{P}(E_{t+1} = 1 | E_t = 1, X_t = 0) = (1 - p_s)(p_{\text{stx}}^0 + p_{\text{stx}}^{d_0}). \quad (13)$$

To obtain $\mathbb{P}(E_{t+1} = 1 | E_t = 1, X_t = 1)$, we simply replace p_s in (13) by q_s . Evidently, the transition probabilities depend on the sampling policy as well as the multiple access scheme.

2) *TCAE [1]*: Building on the real-time reconstruction error metric, we consider the cost of actuation error to capture the significance of the reconstruction error at the point of actuation. To this end, we denote $C_{i,j}$ as the cost of being in state j at the reconstructed source ($\hat{X}_t = j$) when the original source is in state i ($X_t = i$), with $C_{i,i} = 0$. Moreover, we assume $C_{i,j} \neq C_{j,i}$ as different errors have different repercussions on the actuation. Finally, we assume that $C_{i,j}$, $\forall i, j$, is static over the entire observation interval. Following the above discussion, we calculate the TCAE as

$$\bar{C}_A = \pi_{(0,1)} C_{0,1} + \pi_{(1,0)} C_{1,0}, \quad (14)$$

where $\pi_{(i,j)}$, $\forall i, j \in \{0, 1\}$ is obtained from the stationary distribution of the DTMC, describing the joint status of the source state X_t and the reconstruction error state E_t at t .

IV. SAMPLING POLICY AND MULTIPLE ACCESS SCHEMES

In this section we delineate the sampling policy for process monitoring at the intermittent user and highlight its effect on the performance metrics. It should be emphasized that the choice of the sampling policy is closely intertwined with the choice of the multiple access scheme. Keeping this in mind, we consider the semantics-aware sampling policy which triggers sample generation in two cases [1]. First, whenever a change in the state of the source between two consecutive slots is observed, i.e., $X_{t+1} \neq X_t$. Second, when the system is known to be in erroneous state, i.e., $\hat{X}_t \neq X_t$ [1]. Such a policy integrates well with FDMA and NOMA. Moreover, unlike uniform and change-aware sampling policies, the semantics-aware policy requires feedback from the receiver to the transmitter to trigger sample generation [1]. Additionally, feedback is used to re-transmit failed update deliveries. The sampling policy, together with the frame structure, dictates the probability of sampling and transmission events and in turn the value of p_{stx}^j in equations (12) and (13). On the other hand, together with the choice of multiple access scheme, which dictates the probability of successful decoding $p_{2,i,t}$, it determines the value of $p_{\text{stx}}^{d_j}$. To this end, we delineate the calculation of $p_{2,i,t}$ for FDMA and NOMA schemes. We assume the intermittent user has no knowledge of its channel due to its sporadic access behavior and, therefore, always transmits at power P_{max} .

1) *FDMA*: As the users are allocated orthogonal sub-bands, the signal of the intermittent user is not subject to interference from the broadband user. Therefore, $p_{2,i,t}$ for the transmitted packet at time slot t can be calculated from (5), where $\gamma_{2,i,t}$, obtained using (3), will be devoid of the interference term.

2) *NOMA*: Since users share time-frequency resources in NOMA and the capture effect can occur, the successful decoding probabilities of both users' signals at time slot t become interdependent. Therefore, to calculate $p_{i,2,t}$ for the intermittent user, we first define two possible outcomes

- \mathcal{I} : The signal of the intended user gets successfully decoded. Either 1) the signal of the intended user has a sufficiently high SINR to be decoded directly, or 2) the signal from the other user is decoded first, its interference is eliminated using SIC, and then the intended signal has a sufficiently high SNR and gets decoded.
- \mathcal{E} : The signal of the intended user has insufficient SNR to be decoded.

Evidently, the transmission from the intermittent user will get successfully decoded in two cases: $(\mathcal{I}, \mathcal{I})$ and $(\mathcal{E}, \mathcal{I})$, where ordered pairs (\cdot, \cdot) describe possible outcomes for the signals of both users when they overlap. Subsequently, the probability of successful decoding of the signal of the intermittent user can be calculated as $p_{2,i,t} = \pi_{\mathcal{I}\mathcal{I}} + \pi_{\mathcal{E}\mathcal{I}}$, where both $\pi_{\mathcal{I}\mathcal{I}}$ and $\pi_{\mathcal{E}\mathcal{I}}$ can be obtained from Appendix A in [8].

TABLE I
SIMULATION PARAMETERS

Parameter	Symbol	Value
Broadband user erasure probability	ϵ^*	0.1
Broadband user maximum data rate	γ_1^{\max}	5 Mbps
Maximum transmission power	P_{\max}	200 mW
Antenna gains	$G_t G_r$	10
Time slot duration	T_s	1 ms
Carrier frequency	f_c	2 GHz
System bandwidth	B	1 MHz
Noise temperature	T_w	190 K
Noise figure	N_f	5 dB
Frame length	T_F	10
Broadband user source block length	K	32
Intermittent user packet length	L	128 B
BS-intermittent user distance	d	{100, 200, 400} m
Path loss exponent	η	2.6
Cost of actuation error coefficients	$C_{i,j}$	$C_{0,1} = 5, C_{1,0} = 1$

V. RESULTS

In this section, we evaluate the performance of the broadband user and the intermittent user sharing resources in the considered frame-based communication model. Here, the broadband user is located at a distance of 50 m, whereas the intermittent user is located at a distance d from the BS. The system parameters are listed in Table I. To begin with, we analyse the performance of the intermittent user for FDMA frames (i.e., $B_3 = 0$), with increasing value of B_2 . For comparison, we consider the frame-less communication model assumed in conventional studies as the baseline [1]. Such model ‘idealistically’ assumes instantaneous transmission of the updates and feedback, hence, is denoted as the ‘Idealistic’ model throughout this section. The time-averaged reconstruction error, TRE, for the Idealistic model with the semantics-aware sampling policy can be analytically calculated as

$$\bar{E} = \frac{2p_s q_s (1 - p_{2,i,t})}{p_{2,i,t} (p_s + q_s) + 4p_s q_s (1 - p_{2,i,t})}. \quad (15)$$

However, deriving the analytical expression of the TRE for the model in Section II-A, denoted as the ‘Frame-Based’ model, is only tractable for sampling policies that do not require feedback, e.g., uniform and change-aware. This is due to the constraints of the frame structure on the transmission of feedback, discussed in Section II. Since the considered semantics-aware sampling policy requires feedback, deriving an analytical expression similar to (15) for the Frame-Based model becomes intractable. Therefore, we numerically evaluate the performance of the intermittent user in the Frame-Based model by simulating more than 100000 frames.

Fig. 4(a) illustrates the TRE with increasing $B_2 = \{0.1B, 0.2B, \dots, B\}$; for source transition probabilities ($p_s = 0.1, q_s = 0.15$) and distance $d = \{100, 200, 400\}$ m. The relatively small values of p_s and q_s imply that the DTMC source is changing slowly, whereas varying values of d are considered to observe the TRE for varying decoding probabilities. The figure illustrates that the successful decoding probability increases with increasing B_2 and, consequently, the TRE at the BS decreases. Moreover, the farther the intermittent user is from the BS, the larger B_2 needs to be to

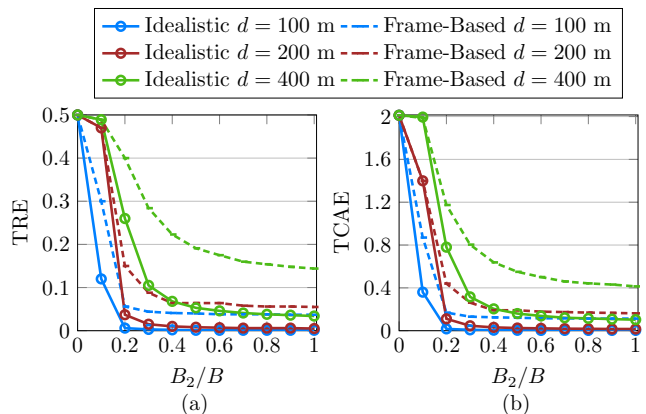


Fig. 4. TRE and TCAE of the intermittent user

reduce the TRE. As expected, with increasing B_2 the decline in TRE is steeper for the Idealistic model. This gets more pronounced with increasing d . However, the performance gain of the Idealistic model over the Frame-Based model comes at the expense of very high UC, as illustrated in Table II for parameters $B_2 = 0.4B$ and $d = 400$. The table shows that while TRE for the Idealistic model is 70% less than that in Frame-Based model, the UC is 134% more. Similar behaviour is observed with the TCAE metric; albeit the difference in performance is narrower, as observed in Fig. 4(b).

The impact of the UC becomes further pronounced in the case of a fast changing DTMC process, as illustrated in Table III that compares the performance metrics of the intermittent user for a slow process ($p_s = 0.1, q_s = 0.15$) and a fast process ($p_s = 0.2, q_s = 0.7$), for $B_2 = 0.4B$ and $d = 400$. It can be observed that as the DTMC process becomes fast changing, both error metrics increase for the Idealistic model. In comparison, for the Frame-Based model, the TRE remains the same and the TCAE decreases. Such discrepancy is by virtue of the fact that delayed feedback is the limiting factor for the Frame-Based model. Therefore, as the process becomes fast changing, it leads to more frequent updates which in turn mitigates the inimical impact of delayed feedback. As a result, while the UC decreases by 16% and 54% for the Idealistic and Frame-Based models, respectively, due to frequent updates, performance metrics degrade for the former model but improve for the latter. Alternatively, the results also suggest that the desired error-metric performance for the Frame-Based model can be achieved by adjusting the frame length, with only a modest change in the UC.

We now analyse the achievable trade-offs between the performance of the broadband user and the intermittent user in the Frame-Based model for the process ($p_s = 0.1, q_s = 0.15$). Fig. 5(a) illustrates the Pareto front vis-à-vis throughput per-

TABLE II
INTERMITTENT USER PERFORMANCE METRICS, $B_2 = 0.4B$ AND $d = 400$

	Idealistic	Frame-Based
TRE	0.068	0.223
TCAE	0.204	0.638
UC	0.614	0.263

TABLE III
PERFORMANCE OF THE INTERMITTENT USER WITH SOURCE VARIABILITY

	Idealistic		Frame-Based	
	Slow Process	Fast Process	Slow Process	Fast Process
TRE	0.068	0.129	0.223	0.250
TCAE	0.204	0.387	0.638	0.550
UC	0.614	0.518	0.263	0.121

formance of the broadband user and TCAE performance of the intermittent user for FDMA frames. The TCAE decreases by virtue of increasing B_2 , hence the throughput performance of the broadband user decreases, as B_1 decreases. It is also evident that with increasing d , the area of the corresponding Pareto front decreases. Nevertheless, it is interesting to observe from Fig. 5(a) that a marginal throughput reduction is needed to accommodate the transmissions of the intermittent user in FDMA and improve its error metrics. However, the throughput drops significantly after a TCAE, which is naturally different for different distances. This is due to the fact that maintaining throughput performance with decreasing B_1 comes at the expense of increasing transmission power by the broadband user. This is reflected in the energy efficiency performance illustrated in Fig. 5(b). A consistent decline in the energy efficiency of the broadband user is observed with decreasing TCAE of the intermittent user. Ultimately, as P_{\max} becomes insufficient to achieve r_1^{\max} ; see equation (8); the throughput performance also starts decreasing; Fig. 5(a).

Next, we focus on the performance of the two users for NOMA frames, i.e., $B_3 = B$. Fig. 5(a) and Fig. 5(b) illustrate that with NOMA, the broadband user achieves high throughput and energy efficiency, whereas the intermittent user achieves a modest TCAE performance. Interestingly, in Fig. 5(b), the performance metrics of both users with NOMA lie outside of the FDMA Pareto front. Specifically, to reduce TCAE by half,

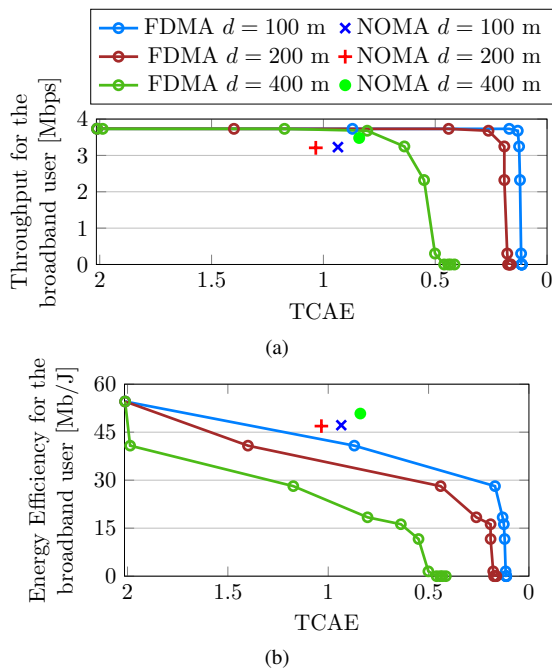


Fig. 5. Throughput and Energy Efficiency performance of the broadband user versus the TCAE of the intermittent user.

TABLE IV
PERFORMANCE OF THE INTERMITTENT USER: FDMA VS. NOMA.

	TCAE		UC	
	FDMA	NOMA	FDMA	NOMA
$D = 100$	0.92	0.94	0.44	0.45
$D = 200$	1.06	1.03	0.54	0.52
$D = 400$	0.84	0.84	0.39	0.38

the drop in energy efficiency with NOMA is significantly less than that with FDMA. Note that, the TCAE of the intermittent user being worst for $d = 200$ is due to small differences between the SNRs of the users leading to low capture probabilities. Regarding UC, Table IV illustrates that NOMA achieves similar TCAE performance to FDMA, without any increase in the UC. Therefore, NOMA achieves a better performance trade-off between the two users.

VI. CONCLUSION

This work investigated and analysed the task-dependent error-metrics performance of a real-time remote tracking and actuation scenario in a Frame-Based resource sharing scenario. A communication model predicated on ‘idealistic’ assumptions in conventional studies on real-time remote reconstruction was considered as the baseline. We demonstrated that the error-metrics performance gain of the baseline model in conventional systems over Frame-Based model is achieved at the expense of a disproportionately high update-delivery cost. After that, for the Frame-Based model, we analysed the performance trade-off between the intermittent user effectuating the real-time remote tracking and a broadband user, for FDMA and NOMA schemes. We demonstrated that NOMA achieves a better performance trade-off between the users, particularly when energy efficiency is the measure for the broadband user. Building on this work, future studies will investigate joint optimization of the sampling policy and the uplink transmit power to improve the performance metrics of both users.

REFERENCES

- [1] M. Salimnejad, M. Kountouris, and N. Pappas, “Real-time reconstruction of markov sources and remote actuation over wireless channels,” *IEEE Transactions on Communications*, vol. 72, no. 5, pp. 2701–2715, 2024.
- [2] J. Weimer, et al., “Distributed event-triggered estimation in networked systems,” in *Proc. IFAC Conference on Analysis and Design of Hybrid Systems*, vol. 45, no. 9, 2012, pp. 178–185.
- [3] Y. Sun, Y. Polyanskiy, and E. Uysal, “Sampling of the wiener process for remote estimation over a channel with random delay,” *IEEE Transactions on Information Theory*, vol. 66, no. 2, pp. 1118–1135, 2020.
- [4] P. Popovski et al., “A perspective on time toward wireless 6G,” *Proceedings of the IEEE*, vol. 110, no. 8, pp. 1116–1146, 2022.
- [5] M. Kountouris and N. Pappas, “Semantics-empowered communication for networked intelligent systems,” *IEEE Communications Magazine*, vol. 59, no. 6, pp. 96–102, 2021.
- [6] N. Pappas and M. Kountouris, “Goal-oriented communication for real-time tracking in autonomous systems,” in *Proc. IEEE Int. Conf. on Autonomous Systems (ICAS)*, 2021, pp. 1–5.
- [7] I. Leyva-Mayorga et al., “Heterogeneous radio access with multiple latency targets,” in *Proc. 57th Asilomar Conf. on Signals, Systems, and Computers*, 2023, pp. 80–84.
- [8] F. Chiariotti et al., “RAN slicing performance tradeoffs: Timing versus Throughput Requirements,” *IEEE Open Journal of the Communications Society*, vol. 3, pp. 622–640, 2022.
- [9] F. Chiariotti, I. Leyva-Mayorga, Č. Stefanović, A. E. Kalør, and P. Popovski, “Spectrum Slicing for Multiple Access Channels with Heterogeneous Services,” *Entropy*, vol. 23, no. 6, p. 686, May 2021.